

Adaptive Reticulum

Giuseppe Nuti, Lluís Antoni Jiménez Rugama,
Kaspar Thommen

April 18, 2022

Abstract

Neural Networks and Random Forests: two popular techniques for supervised learning that are seemingly disconnected in their formulation and optimization method, have recently been linked in a single construct. The connection pivots on assembling an artificial Neural Network with nodes that allow for a gate-like function to mimic a tree split, optimized using the standard approach of recursively applying the chain rule to update its parameters. Yet two main challenges have impeded wide use of this hybrid approach: *(a)* the inability of global gradient descent techniques to optimize hierarchical parameters (as introduced by the gate function); and *(b)* the construction of the tree structure, which has relied on standard decision tree algorithms to learn the network topology or incrementally (and heuristically) searching the space at random. We propose a probabilistic construct that exploits the idea of a node’s *unexplained potential* (the total error channeled through the node) in order to decide where to expand further, mimicking the standard tree construction in a Neural Network setting, alongside a modified gradient descent that first locally optimizes an expanded node before a global optimization. The probabilistic approach allows us to evaluate each new split as a ratio of likelihoods that balance the statistical improvement in explaining the evidence against the additional model complexity — thus providing a natural stopping condition. The result is a novel classification and regression technique that leverages the strength of both: a tree-structure that grows naturally and is simple to interpret with the plasticity of Neural Networks that allow for soft margins and slanted boundaries.

1 Introduction

Both Random Forests (RF) and Neural Networks (NN) are popular techniques ubiquitous in the Machine Learning world. NN tend to excel at vision and speech recognition, whilst RF work best in classification problems where specific subregions of the input space are associated with a different likelihood of belonging to one class (think of a heart attack risk analysis, where having a high resting heart-rate *and* being older than 50 significantly increases the probability of a coronary disease).

Interestingly, the two techniques are complementary in that the shortcomings of one tend to be the advantages of the other. NN provide for soft margin hyperplanes (thanks to the sigmoidal activation function) and all of the parameters are optimized at once (albeit potentially resulting in a local optima); the main drawbacks are that (*a*) the topology of the network is fixed and designed by an expert, although recent studies do cover various approaches to either pruning or growing a network (notably in [1] and more generally reviewed in [2]), alongside an analysis of the theoretical bounds when introducing a regularization penalty based on the complexity of the network (in [3]); and (*b*) the network is most often a black box where the prediction is not readily understandable by inspecting the network's trained parameters. Conversely, RF allow for a natural method to incrementally define the structure of each tree, (and where each single tree can generally be interpreted, depending on its depth). Arguably, the main disadvantages of RF are: (*a*) the inability to define a soft and slanted margin for the split (as the standard tree/random-forest boundaries are limited to a single variable per split); and (*b*) the step-wise greedy nature of the optimization where splits closer to the root are not optimized in light of newer splits (a shortcoming that a chessboard-like dataset easily illustrates).

As we look to join decision trees and NN, the obvious challenge is in how to grow the network topology to mimic the simple and effective approach in trees (which employ an exhaustive search across all possible segmentation along the input dimensions — yet without the ability to add an angle to the separating hyperplane). The challenge in growing a NN like a tree pivots on knowing which leaf to expand and assessing if an expansion has provided a statistically significant improvement in our model of the data — both inextricably linked to understanding the likelihood of the data with respect to our model. As such, we introduce a key modification to the cost function of the NN: since the tree-like formulation allows us to know the probability that an observation belongs to a particular leaf, we can simply use the

posterior probability of the data (given the probability of belonging to each leaf). This has a closed form derivation for many distributions (including all the distributions in the exponential family, as detailed in [4], for example). Notably, this approach removes all of the free parameters from the leaf nodes, which traditionally have had the same formulation as inner nodes (e.g. a sigmoid activation function for classification problems, etc.)

This new formulation allows us to tackle both of the key aspects of generating a network topology: firstly, we can prioritize expanding nodes where the probability of the data is low. Imagine a leaf node that is fully explained, i.e. where all of the points belong to the same class: there would be no point in further expanding it (and equally a leaf with very few data points is unlikely to yield a large improvement in the model). Conversely, a leaf with many heterogeneous points is a great candidate for further expansion. We call this the *unexplained potential* of each leaf, which determines how likely we are to pick a leaf for expansion. Once we have expanded a node, we can examine each leaf versus its parent (by comparing the log-likelihood of the two leaves against the log-likelihood of the parent): we expect the data to be better explained by the additional complexity, with the Bayesian approach ensuring that we have sufficient statistical evidence to support the expansion. Finally, a word on explainability: as this topic gathers momentum in the Machine Learning world (see [5] for a recent study), we transform the standard formulation for the separating hyperplane (traditionally in Cartesian coordinates) into its Polar coordinates equivalent. This allows us to better understand the model (upon visual inspection) and to remove the need to regularize the weights as the Polar approach explicitly defines the stiffness of the sigmoid around the separating hyperplane.

The idea of a tree expressed as a NN has been explored in various recent works: for example, in [6] and [7], where Tanno *et al.* provide an adaptive hybrid model that uses both gate-like functions and standard NN components (alongside a review of similar approaches). The work by [7] allows for the network topology to grow incrementally randomly choosing a node to extend (and if to extend it via gate or a standard NN transformation). Previously, the idea of using back-prorogation for Decision Trees via a soft margin is studied by Medina-Chico *et al.* in [8]. Biau *et al.* in [9] exploit the structure derived from a standard Random Forest algorithm to train a NN-equivalent formulation (with soft margin and slanted hyperplanes), which have also been proposed in [10] and [11], where the optimization of the parameters can be either via back-propagation (in [10]) or as a global integer problem (in [11]).

Finally, setting the construction of a NN in probabilistic terms has received attention of late (beyond the use of the log-likelihood as a loss function), using either Markov Chain Monte Carlo methods (as in [12]) and Variational Bayes (in [13]), both more generally reviewed in [14]. Separately, Chouikhi and Alim in [15] explore the use of the Beta function instead of the more common sigmoid activation function. Bayesian Decision Trees in [16] are a fully probabilistic formulation of the data and tree-generation process and share the theoretical approach with this work.

2 Adaptive Bayesian Reticulum

Our overall objective is to estimate the probabilities of an outcome y given the input \mathbf{x} , namely $p(y|\mathbf{x})$. Our approach is based on a soft version of the Bayesian Decision Trees from [16] which leverages the optimization approach of neural networks.

Decision Trees are hierarchical models represented by nodes and edges. In general, Trees contain two types of nodes, internal nodes $n \in \mathcal{N}$, and terminal nodes $\ell \in \mathcal{L}$ also called leaves. We will assume all Trees are binary (though one may use other types of trees). An important property of the Trees is that, except for the root node n_0 , all nodes have a unique parent. Furthermore, all internal nodes have two children connected with an edge. More specifically, Decision Trees are those Trees whose internal nodes contain a rule activating one of the children depending on \mathbf{x} . We name these rules the gate function g_j at node n_j , which only takes values $\{0, 1\}$, defined such that the *left* child is activated when $g_j(\mathbf{x}) = 1$, and the *right* child is activated when $1 - g_j(\mathbf{x}) = 1$. Figure 2.1 provides an example of a Decision Tree with three internal nodes and four leaves.

To model the probability $p(y|\mathbf{x})$ using a Decision Tree we define the following,

- (a) $p(\mathbf{x} \in \ell)$: probability that an input \mathbf{x} belongs to the leaf ℓ ;
- (b) $p(y|\mathbf{x} \in \ell)$: probability of an outcome y given that the input \mathbf{x} belongs to the leaf ℓ .

We can use these probabilities to rewrite $p(y|\mathbf{x})$,

$$p(y|\mathbf{x}) = \sum_{\ell \in \mathcal{L}} p(y|\mathbf{x} \in \ell)p(\mathbf{x} \in \ell). \quad (2.1)$$

Within a Decision Tree, the probability $p(\mathbf{x} \in \ell)$ is the product of all gate functions that connect the root n_0 to the leaf ℓ . For instance, in the example from Figure 2.1, $p(\mathbf{x} \in \ell_1) = g_0(\mathbf{x})g_1(\mathbf{x})$, $p(\mathbf{x} \in \ell_2) =$

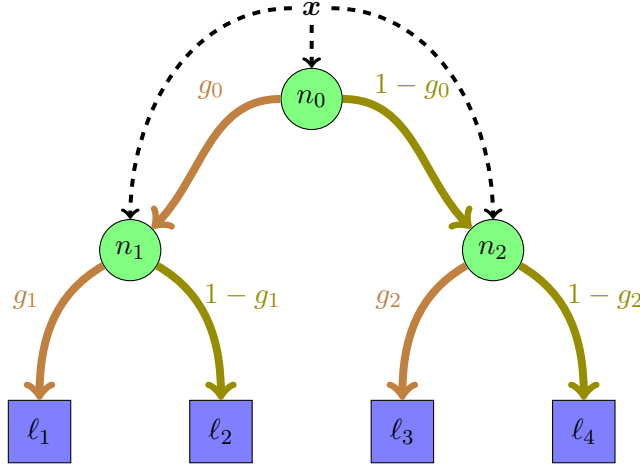


Figure 2.1: A decision tree with three internal nodes $\mathcal{N} = \{n_0, n_1, n_2\}$ and four leaves $\mathcal{L} = \{\ell_1, \ell_2, \ell_3, \ell_4\}$.

$g_0(\mathbf{x})(1 - g_1(\mathbf{x}))$, $p(\mathbf{x} \in \ell_3) = (1 - g_0(\mathbf{x}))g_2(\mathbf{x})$, and $p(\mathbf{x} \in \ell_4) = (1 - g_0(\mathbf{x}))(1 - g_2(\mathbf{x}))$. Notice that $p(\mathbf{x} \in \ell)$ only takes values 0 or 1. The probability $p(y|\mathbf{x} \in \ell)$ is defined per leaf and described in Section 2.1.

More generally, Decision Trees can be defined as a one layer neural network that includes the tree hierarchical structure constraints, [9]. In both cases, the gate function for a node n_j is defined by a manifold \mathcal{M} such that $g_j(\mathbf{x}) = s(d_{\mathcal{M}}(\mathbf{x}))$. For this gate function, $d_{\mathcal{M}}(\mathbf{x})$ is a signed distance from \mathbf{x} to \mathcal{M} , and s , called the activation function, transforms a real value into a number between 0 and 1. In this article, we only consider \mathcal{M} to be from the set of affine hyperplanes, i.e. for a hyperplane with weights \mathbf{w} , we choose $d_{\mathcal{M}}(\mathbf{x}) = w_0 + \sum_{k=1}^d w_k x_k$. Decision Trees are built with the Heaviside function $s(x) = \mathbb{1}_{\{x>0\}}$ for activation. Crucially, a smooth s allows to soften the Decision Trees, i.e. $p(\mathbf{x} \in \ell)$ can take any value between 0 and 1, in order for us to optimize the parameters leveraging the back-propagation concepts from neural networks, [17].

In soft Decision Trees, the value $p(\mathbf{x} \in \ell)$ is the probability that the outcome y of \mathbf{x} was generated by the distribution of leaf ℓ . As a shorthand, we will keep the notation of \mathbf{x} belonging to ℓ .

2.1 Bayesian Reticulum

We can now define a Bayesian Reticulum¹ for binary classification problem (regression and multiclass classification problems can naturally be extended from the definitions below). We will assume we have a set of points $\{\mathbf{x}_i\}_{i=1}^m$ in \mathbb{R}^d with outcomes $\{y_i\}_{i=1}^m$ in $\{0, 1\}$. The number of dichotomies into which \mathbf{w} can separate $\{\mathbf{x}_i\}_{i=1}^m$ differently is known, [18]. If we assign a value to each dichotomy, an exhaustive search for an optimal dichotomy is not feasible for two reasons: the number of possible dichotomies increases exponentially with m , and identifying each dichotomy is hard. The problem becomes yet more complex when we consider a Decision Tree involving more than one hyperplane. As such, we propose a solution that consists on relaxing the activation function of Decision Trees to apply a gradient ascent algorithm.

A Reticulum is a Decision Tree whose gate functions take the form $g(\mathbf{x}) = (1 + e^{-(w_0 + \sum w_k x_k)})^{-1}$. In other words, we only consider affine hyperplanes and choose s to be the sigmoid function. The Bayesian Reticulum is a Reticulum where we defined the expected log-likelihood and the expected $p(y|\mathbf{x} \in \ell)$ for each leaf given the input data, as introduced in [16].

Because each point \mathbf{x} has a different probability of belonging to each leaf, there are $|\mathcal{L}|^m$ different possible outcomes. Let's denote the outcomes by $\omega \in \Omega$ where ω maps point i to leaf $\omega(i)$. Then, each ω has a probability $p(\omega) = \prod_i p(\mathbf{x}_i \in \omega(i))$ of occurring. If α and β are the parameters for the Beta conjugate prior, we can obtain the posterior parameters for leaf ℓ and configuration ω ,

$$\begin{aligned}\alpha'_\ell(\omega) &= \alpha + \sum_{i=1}^m \mathbb{1}_{\{\omega(i)=\ell\}}(1 - y_i), \\ \beta'_\ell(\omega) &= \beta + \sum_{i=1}^m \mathbb{1}_{\{\omega(i)=\ell\}} y_i.\end{aligned}$$

The expected marginal log-likelihood for the Bayesian Reticulum is,

$$\begin{aligned}\mathbb{E}_\omega \left[\sum_{\ell \in \mathcal{L}} \ln \left(\frac{B(\alpha'_\ell(\omega), \beta'_\ell(\omega))}{B(\alpha, \beta)} \right) \right] \\ = \sum_{\omega \in \Omega} \sum_{\ell \in \mathcal{L}} \ln \left(\frac{B(\alpha'_\ell(\omega), \beta'_\ell(\omega))}{B(\alpha, \beta)} \right) p(\omega), \quad (2.2)\end{aligned}$$

¹Loosely inspired by an *endoplasmic reticulum*, a component of organic cells. Bayesian reticula are similar in structure to endoplasmic reticula in that they both grow organically with occasional consolidation (purging) of structural elements.

where B is the Beta function. Similarly, the expected probabilities at each leaf are,

$$\begin{aligned} p(y = 0 | \mathbf{x} \in \ell) &= \sum_{\omega \in \Omega} \frac{\alpha'_\ell(\omega)}{\alpha'_\ell(\omega) + \beta'_\ell(\omega)} p(\omega), \\ p(y = 1 | \mathbf{x} \in \ell) &= \sum_{\omega \in \Omega} \frac{\beta'_\ell(\omega)}{\alpha'_\ell(\omega) + \beta'_\ell(\omega)} p(\omega). \end{aligned} \quad (2.3)$$

Note that the probabilities in equation (2.3) are not free parameters and are fully determined by $p(\mathbf{x}_i \in \ell)$ and y_i (unlike standard NN where the last layer is parametrized as the *de facto* probability of belonging to a class and optimized within the gradient ascent).

Our goal is to find the optimal Bayesian Reticulum given the input data, i.e. maximize equation (2.2). The summation over $|\mathcal{L}|^m$ is not computationally feasible: as such, we optimize a lower bound of (2.2). Because the log-beta function is convex, [19], we apply Jensen's inequality [20] and obtain,

$$c = \sum_{\ell \in \mathcal{L}} \ln \left(\frac{B(\alpha'_\ell, \beta'_\ell)}{B(\alpha, \beta)} \right), \quad (2.4)$$

with

$$\begin{aligned} \alpha'_\ell &= \mathbb{E}_\omega [\alpha'_\ell(\omega)] = \alpha + \sum_{i=1}^m p(\mathbf{x}_i \in \ell)(1 - y_i), \\ \beta'_\ell &= \mathbb{E}_\omega [\beta'_\ell(\omega)] = \beta + \sum_{i=1}^m p(\mathbf{x}_i \in \ell)y_i. \end{aligned}$$

The probabilities at each leaf can also be approximated,

$$\begin{aligned} p(y = 0 | \mathbf{x} \in \ell) &= \frac{\alpha'_\ell}{\alpha'_\ell + \beta'_\ell}, \\ p(y = 1 | \mathbf{x} \in \ell) &= \frac{\beta'_\ell}{\alpha'_\ell + \beta'_\ell}. \end{aligned} \quad (2.5)$$

Finally, we define the value $c_\ell = \ln(B(\alpha'_\ell, \beta'_\ell)/B(\alpha, \beta))$ as the leaf *unexplained potential* — i.e. the lower bound on the (log) probability of the data at a particular leaf (which will be useful as we look to explore which leaf to expand further). The intuition behind this definition is that the smaller the value of c_ℓ , the more likely we are to find a new set of weights \mathbf{w} at leaf ℓ that improve the Reticulum expected log-likelihood.

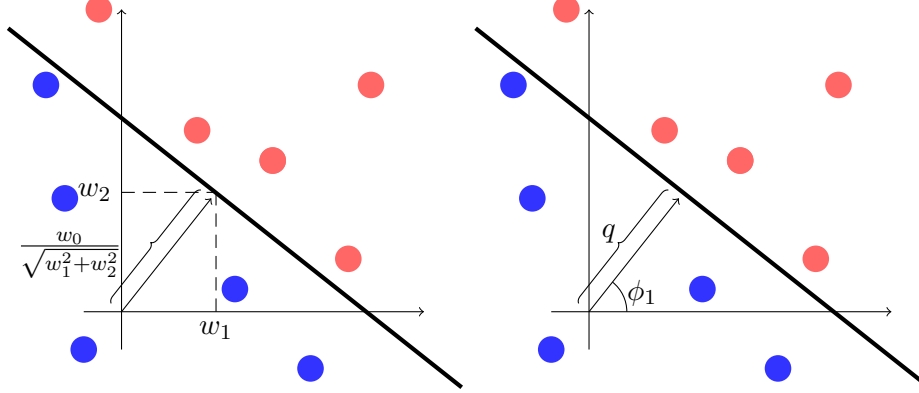


Figure 2.2: A hyperplane defined in Cartesian coordinates on the left, and polar coordinates on the right. While in Cartesian coordinates we define the hyperplane as $w_0 + w_1x_1 + w_2x_2 = 0$, in polar we can write $q + \cos(\phi_1)x_1 + \sin(\phi_1)x_2 = 0$.

2.2 Neural Networks in Polar Coordinates

In a bid to make the model explainable, we note that the node weights \mathbf{w} have a geometrical interpretation. For a hyperplane $w_0 + \sum_{k=1}^d w_k x_k = 0$, the weights w_1, \dots, w_d define the orthogonal direction to the hyperplane, and w_0/r defines the distance or location of the hyperplane to the origin, $r = \sqrt{\sum_{k=1}^d w_k^2}$.

The Euclidean distance of a point \mathbf{x} to the hyperplane defined by \mathbf{w} is $|w_0 + \sum w_k x_k|/r$. This is related to the signed distance introduced in Section 2, $d_{\mathcal{M}}(\mathbf{x}) = w_0 + \sum w_k x_k$. If we disregard the sign, $d_{\mathcal{M}}(\mathbf{x})$ is the Euclidean distance times r . This scaling is not accidental and defines the softness of our gate function margin. Note that a large scaling will transform the sigmoid s into a Heaviside function.

Any change in w_1, \dots, w_d will cause a change in the direction, location, and scaling r of the hyperplane. Because the scaling is not required to define the hyperplane, we propose the polar coordinates substitution from Appendix C. This substitution allows to adjust the scaling, location, and direction of the hyperplane independently². Figure 2.2 shows how a hyperplane in \mathbb{R}^2 is defined in Cartesian and polar coordinates.

²Indeed, our original motivation to explore the polar coordinates approach was to enable a fully Bayesian treatment of the prior parameters of a Neural node which, in the case of the standard Cartesian form, would have to be defined as an unnecessarily complex joint probability distribution over all possible \mathbf{w} instead of an independent distribution for each angle.

2.3 Construction of Bayesian Reticula

The main objective in constructing a Bayesian Reticula is to maximize the bound c from equation (2.4). We do not assume any *a priori* knowledge of the structure of the Reticulum. Instead, we discover the structure adaptively based on the input data. During this construction, we will attempt to extend randomly selected leaves by sampling and optimizing new node weights for these leaves.

We provide the general algorithm to construct Bayesian Reticula in Algorithm 1. First, we initialize the Reticulum starting at the root node (leaf). As the number of leaves grows, we choose the leaf we want to extend proportionally to the unexplained potential,

$$\frac{c_\ell}{\sum_{j=1}^{|L|} c_{\ell_j}}, \quad \text{for leaf } \ell. \quad (2.6)$$

For the chosen leaf, we sample the weights uniformly over the unit sphere and locally optimize the weights, keeping the rest of the network parameters constant. After the local optimization, we perform a global optimization³ and finally, assess every leaf to determine whether it should be pruned. In other words, we keep those leaves that improve the marginal log-likelihood with respect to their parent by a minimum amount. Figure 2.3 shows an example of a partially constructed Reticulum.

Algorithm 1 Construction of Bayesian reticula.

```

1: procedure CONSTRUCT
2:    $a \leftarrow 0$ , initialize reticulum
3:   while  $a < \text{max\_attempts}$  do
4:      $j \leftarrow$  choose index of node to extend
5:     Sample weights for node  $j$ 
6:     Train the reticulum using a gradient ascent algorithm
7:     Prune the reticulum
8:      $a \leftarrow a + 1$ 
9:   end while
10: end procedure

```

The construction of Reticula is sensitive to steps 4 to 7. In particular, the gradient ascent convergence properties will affect the effectiveness of Algorithm 1. As discussed in the previous section, these

³The log-likelihood function of the Bayesian Reticulum defined in equation (2.4) is differentiable with respect to the node weights. Thus, one can apply any gradient ascent algorithm to optimize the weights. As proposed for neural networks, [17], we provide the details of a back-propagation algorithm in Appendix B.

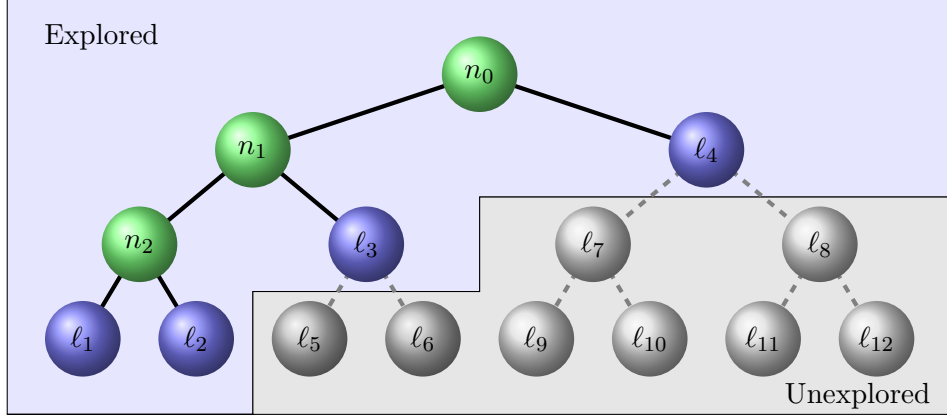


Figure 2.3: Reticulum with a maximum of four levels. At this stage, we extended nodes n_0, n_1 , and n_2 . The current leaves are ℓ_1, ℓ_2, ℓ_3 , and ℓ_4 . Because there is a maximum of four levels, only ℓ_3 and ℓ_4 can be extended. The gray region of the reticulum has not been explored yet.

properties are easier to explain in polar coordinates (see Appendix C for the re-parametrization). As such, we define r as the *stiffness* of a node, which is soft when r is small, and stiff when r is large.

In practice, if a node is stiff the sigmoid s has been scaled to look like the Heaviside activation function. In this case, the value s for a point i and node j , namely s_j^i , becomes 0 or 1 and the gradient is close to $\mathbf{0}$, see equation (B.1). When r is small, the sigmoid becomes flatter, centered around 1/2. For soft nodes, the values of s_j^i are close to 1/2 and the gradient values for all coordinates but r are close to 0. Intuitively, all points have equal weights and the most sensitive variable to the Reticulum c is the stiffness.

Furthermore, the hierarchical structure of the Reticulum causes lower level nodes to have a smaller impact on c as opposed to upper level nodes. For instance, the value of g_0 affects $p(\mathbf{x} \in \ell)$ for all leaves while g_1 only affects the leaves on the left of n_0 . If we perform a global gradient ascent optimization to the Reticulum, we observe three important convergence situations: 1) the lower level nodes will barely move with respect to the upper level nodes, 2) stiff nodes will not move, and 3) soft nodes need to stiffen before finding a hyperplane that improves the unexplained potential c_ℓ . To overcome these issues, the training step in line 6 is performed in two phases. First, we perform a local optimization by only updating the current extended node weights. Second, we finish with a global optimization that accounts for all nodes. The first phase is the optimization that regular Decision Trees perform,

while the second is what neural networks perform. This is what places the Reticula as a mixture of both techniques.

After each node extension, we verify whether all nodes are still relevant. Starting from the parents whose children are both leaves, we verify that the sum of the children’s unexplained potentials is better than their parent unexplained potential, i.e. without the split. If the siblings’ value did not improve the parent value by a minimum factor, we prune the parent by setting it to a leaf and repeat the process. In some cases, during the global optimization, points can move from one leaf to another leaving some empty leaves. These empty leaves are an example where a parent would be pruned because the split does not improve the parent’s unexplained potential.

We provide a detailed view for the implementation of Algorithm 1 in Appendix A.

3 Results

We first apply the Reticula to three examples we can visually explain: the recovery of a soft sphere \mathbb{S}^1 , the recovery of a cross, and the Ripley data set [21]. Then, we provide the results that compare the Bayesian Reticula to other similar techniques. In each case we use the parameters from Appendix A.

3.1 Recovery of a Sphere

In this example we train a Reticulum with 5 000 points generated under $\mathbf{X} = ((1 + 0.3N) \cos(2\pi U), (1 + 0.3N) \sin(2\pi U))^t$, where $U \sim \text{Uniform}(0, 1)$ and $N \sim \text{Normal}(0, 1)$ are independent. The outcome Y follows a Bernoulli distribution with probability p . This probability is a function of the Euclidean distance between \mathbf{X} and \mathbb{S}^1 , namely $p = 1/(1 + e^{-10\|\mathbf{X}\|_2})$.

In addition, we use the same points to train 50 random forest trees and a one hidden layer neural network with 30 nodes using the Python Scikit-Learn package, [22]. Figure 3.1 shows the resulting models after training the data set. The final Bayesian Reticulum extended 20 nodes and the in-sample accuracies were 91.8% for the random forest, 84.4% for the Bayesian Reticulum, and 78.1% for the neural network.

For this case, where the solution is smooth and there is not much noise, the neural network finds an accurate shape of \mathbb{S}^1 . The random forest does find a circle although tends to overfit the boundary. The Bayesian Reticulum approximates the circle with straight lines. Depending on the prior strength, the highest and lowest probabilities will adjust.

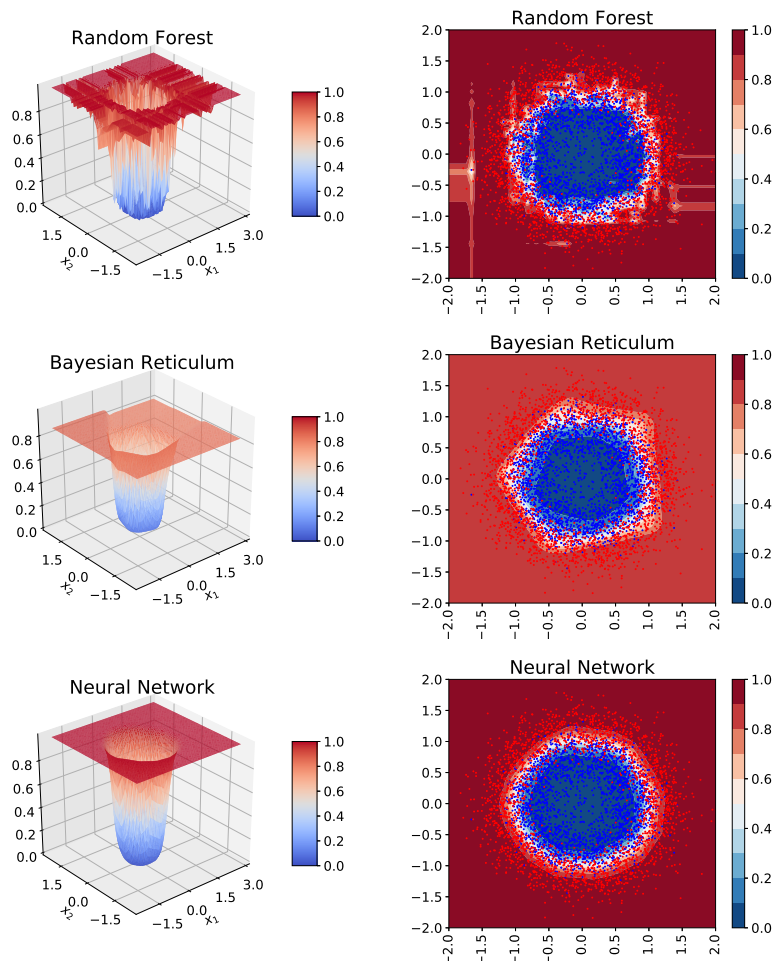


Figure 3.1: Final models obtained training the circle data set with 50 trees in random forests, the Bayesian Reticulum with 20 nodes, and a neural network with one hidden layer of 30 nodes. The legend colors indicate the probability of belonging to the red class.

3.2 Recovery of a Cross

The location of the data for this test is generated uniformly in $[-2, 2] \times [-2, 2]$, i.e. $\mathbf{X} = (U_1, U_2)^t$ with two independent $U_1, U_2 \sim \text{Uniform}(-2, 2)$. Given the locations of 1 000 points, the outcomes Y are sampled from a Bernoulli distribution whose probability is 0.9 in the first and third quadrants, and 0.1 otherwise.

As in the previous example, we compare the trained Bayesian Reticulum to the resulting 50 random forest trees and one hidden layer neural network with 30 nodes. The final Bayesian Reticulum extended 13 nodes and the in-sample accuracies were 93.2% for the random forest, 90.0% for the Bayesian Reticulum, and 78.5% for the neural network. These models are shown in Figure 3.2.

In this example, the noise causes either the random forest and the neural network to overfit the model, i.e. they find additional patterns that do not explain the generation of the data. The Bayesian nature of the Reticulum helps with the model recovery for noisy data.e not

3.3 Ripley Data Set

The Ripley data set, [21], is a 2-dimensional 2-class data set generated using a mixture of two Gaussian distributions. This data set provides a train and a test set. The accuracy of the Bayesian Reticulum applied to this example is 90.2% and the final Reticulum contained 7 nodes. Figure 3.3 provides the model obtained after training, overlapped by the training data.

The resulting model shown in Figure 3.3 is smooth as opposed to Decision Trees. In addition, one can observe two teeth that may explain the existence of four different Gaussian means, two per class in the Gaussian mixture. Figure 3.4 displays how are the first 3 nodes of the Bayesian Reticulum found using Algorithm 1.

3.4 Comparison to Similar Techniques

In [23], the accuracy and model node count is compared for the C4.5 algorithm, the Linear Discriminant Trees (LDT), the Soft Decision Trees (Soft), and the Budding trees (Bud). We provide the same results in Tables 1 and 2, and compare them to the Bayesian Reticula. The highest accuracy model is highlighted using a bold font for either table. The results provide the average accuracy and node count for a 3-fold cross validation. We chose the data sets that did not need any feature manipulation and were accessible to the public: MAG [24], RIN [25], SPA [26], and TWO [27].

The prior distribution of the Bayesian Reticulum is an important parameter of the model. It allows the user to introduce any prior

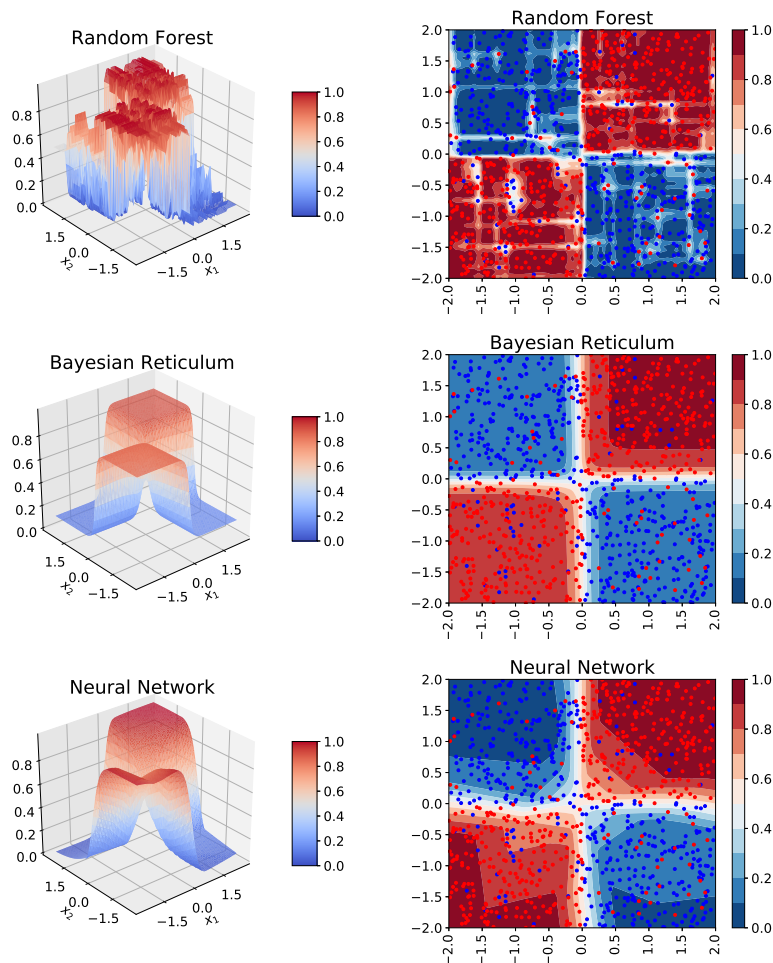


Figure 3.2: Final models obtained training the circle data set with 50 trees in random forests, the Bayesian Reticulum with 13 nodes, and a neural network with one hidden layer and 30 nodes. The legend colors indicate the probability of belonging to the red class.

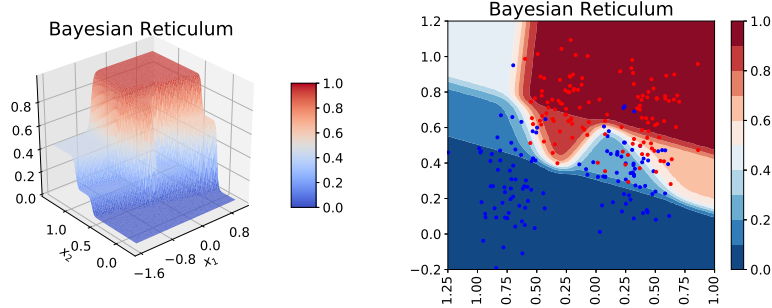


Figure 3.3: The Bayesian Reticulum resulting from training on the Ripley data set. The blue and red circles determine the training data set with outcomes 0 and 1 respectively. The legend colors indicate the probability of belonging to the red class.

	C4.5	LDT	Soft	Bud	Reticulum
MAG	82.5%	83.0%	85.3%	86.3%	85.7% (#2)
RIN	87.7%	77.2%	90.1%	88.5%	89.5% (#2)
SPA	90.0%	89.8%	92.4%	91.4%	93.3% (#1)
TWO	82.9%	98.0%	97.9%	96.7%	97.3% (#3)

Table 1: Resulting 3-fold accuracy for each technique and data set. The best value is highlighted in bold. The Reticulum is ranked in parenthesis.

	C4.5	LDT	Soft	Bud	Reticulum
MAG	53	38	56	122	26.7
RIN	93	3	76	61	21.3
SPA	36	13	12	49	21.7
TWO	163	3	7	29	19.0

Table 2: Resulting 3-fold node count for each technique and data set. The best accuracy model is highlighted in bold.

knowledge of the data generation process which includes the noise level. A data set expected to be separable requires weak prior parameters while a noisy data set requires a strong set of prior parameters to avoid overfitting. The results from Tables 1 and 2 are obtained using the parameters from Appendix A. However, the number of nodes in each resulting Reticulum is sometimes overfitted. By adjusting the prior strength, t in Appendix A, we can obtain similar accuracies with simpler models, as shown in Table 3. In general, the Bayesian Reticu-

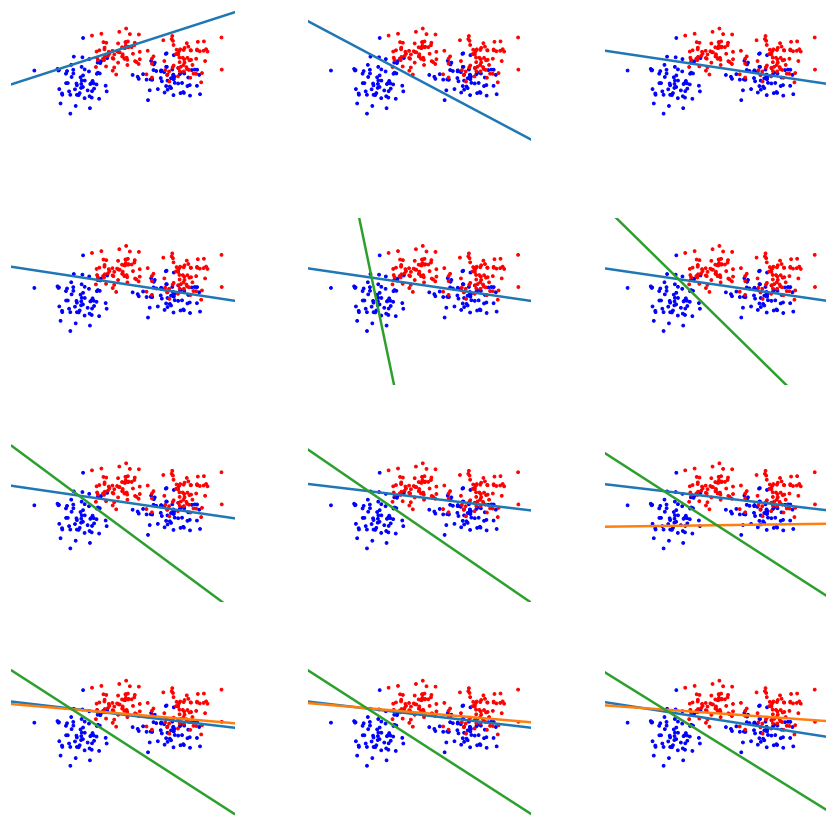


Figure 3.4: Construction of a Bayesian Reticulum for the Ripley training data set. From left to right and top to bottom, the resulting Reticulum every 50 gradient steps. The figure shows the extension of the first three nodes of the Bayesian Reticulum.

lum appears to be among the top techniques in terms of accuracy with a lower number of nodes.

	t	Accuracy	Node count
MAG	0.02	85.6% (#2)	20.7
RIN	0.02	89.3% (#2)	20.7
SPA	0.10	93.0% (#1)	9.3
TWO	0.20	97.8% (#3)	3.7

Table 3: Resulting 3-fold node count after adjusting the prior strength to avoid overfitting.

4 Conclusive Remarks

Bridging RF and NN exposes a number of interesting aspects of both models alongside a novel classification technique that has the advantages of both: a soft tree structure that can be extended (and pruned) iteratively with slanted hyperplanes optimized via gradient ascent, first locally, than globally.

One of the key concept is the idea of a node’s unexplained potential to guide the search of the optimal topology, moving us closer to being able to model a simple problem with a simple topology (following Occam’s Razor). In our opinion this will likely be one of the most interesting areas of research, where the unexplained potential is but one of the important aspects of automatically building a network, such as which two nodes to connect (in the standard NN formulation) and how to model cyclical graphs. Furthermore, we show how the use of the beta function to regularize the model gives a natural stopping condition to the search for a more complex topology which accounts for the available statistical evidence (albeit via an approximation that can most likely be improved).

Finally expressing the standard NN formulation in Polar coordinates allows for a more explainable model, at least in the tree formulation with a gate function. More generally, expressing the problem in Polar coordinates enables us to directly model the angle(s) of the hyperplane, its intercept and the stiffness of the sigmoid curve — opening an interesting area of research for explainable NNs.

A Implementation Details

The input data is normalized before training by removing the average and dividing by the standard deviation at each dimension. The prior parameters are automatically defined by t , called the prior strength. If the input data has m_0 points for class 0 and m_1 points for class 1, the prior parameters are defined as $\alpha = tm_0$ and $\beta = tm_1$. The value of t defines the prior pseudo-count with respect to the input data set size $m = m_0 + m_1$. We use $t = 0.01$ by default.

We implement the Reticulum in array form. Starting at $j = 0$, the parent to children index map is $2j+1$ for the left child, and $2j+2$ for the right child. Given the current extensible leaves, we sample them with their probabilities defined by equation (2.6). Once the leaf is chosen, we generate \mathbf{w} following a uniform distribution over the hyper-sphere. The value of w_0 is randomized using another Gaussian distribution with $\sigma^2 = 1$ and centered around the average distance, weighted by $p(\mathbf{x}_i \in \ell)$. Then, we convert \mathbf{w} into polar coordinates, Appendix C, and set the initial stiffness to $r = 10$. By default, we extend 50 nodes and use 200 gradient iterations for each node. During the gradient phase, half of the steps are performed for the local optimization, and the other half for the global optimization. Finally, the tree is pruned with a factor of $1.05^{\text{level}+1}$, i.e. we prune the children whenever the sum of their values c_ℓ is not better than its parent c_ℓ plus $\ln(1.05^{\text{level}+1})$.

The gradient algorithm we apply is the Newton-Raphson algorithm with an initial step size of 0.1. If the step did not improve the cost c , we reduce the step size by 1/2 and try the new step from the previous location. Otherwise, we increase the step size by 3/2 up to 0.1.

B Backpropagation

Our goal is to maximize equation (2.4). We provide its gradient in order to apply a gradient ascent algorithm. The derivative of c_ℓ with respect to the weight $w_{k,u}$ is,

$$\frac{\partial c_\ell}{\partial w_{k,j'}} = \sum_{z,i,j} \frac{\partial \ln(B)}{\partial z} \frac{\partial z}{\partial s_j^i} \frac{\partial s_j^i}{\partial w_{k,j'}}.$$

In the summation above, $z \in \{\alpha', \beta'\}$, $i = 1, \dots, m$, and j is the node index. We use the notation $w_{k,j'}$ to indicate the weight for dimension k and node index j' . Similarly, we will also use $x_{k,i}$ to indicate the coordinate value of dimension k for point \mathbf{x}_i .

The derivative of $\ln(B)$,

$$\frac{\partial \ln(B)}{\partial z} = \psi(z) - \psi(\alpha' + \beta'),$$

where ψ is the digamma function. Then,

$$\frac{\partial z}{\partial s_j^i} = \begin{cases} \frac{\partial p(\mathbf{x}_i \in \ell)}{\partial s_j^i} (1 - y_i) & \text{if } z = \alpha', \\ \frac{\partial p(\mathbf{x}_i \in \ell)}{\partial s_j^i} y_i & \text{if } z = \beta'. \end{cases}$$

The derivative $\partial p(\mathbf{x}_i \in \ell)/\partial s_j^i$ is 0 if j is not the index of a predecessor of ℓ . Otherwise, it is $p(\mathbf{x}_i \in \ell)/s_j^i$ if j is the index of a left child, or $-p(\mathbf{x}_i \in \ell)/s_j^i$ if j is the index of a right child. Note that $p(\mathbf{x}_i \in \ell)/s_j^i$ can be computed as $p(\mathbf{x}_i \in \ell)$ omitting the weight corresponding to s_j^i . According to the mapping described in Appendix A, to verify whether j corresponds to a left or a right child, one can simply verify whether j is an odd number. Finally,

$$\frac{\partial s_j^i}{\partial w_{k,j'}} = \begin{cases} s_j^i (1 - s_j^i) x_{k,i} & \text{if } j = j', \\ 0 & \text{otherwise.} \end{cases} \quad (\text{B.1})$$

We can perform a backpropagation in three steps: 1) we start at the root, i.e. $j = 0$, and move forward to compute $p(\mathbf{x}_i \in \ell)/s_j^i$ for each node; 2) once a leaf is reached, we can compute and return $(1 - y_i)\partial \ln(B)/\partial \alpha' + y_i\partial \ln(B)/\partial \beta'$; 3) we move backwards, and compute the sum of the left and right children weighted by $p(\mathbf{x}_i \in \ell)/s_j^i$, and $-p(\mathbf{x}_i \in \ell)/s_j^i$ respectively. This sum is used to complete the partial derivatives with respect to the weights at j . We return the sum of the children weighted by s_j^i and $1 - s_j^i$ respectively to account for the weights s_j^i in the derivatives of the predecessors of j .

C Polar Coordinates

Given the weights \mathbf{w} , we provide a particular substitution based on polar coordinates,

$$\begin{aligned} w_0 &= qr, \\ w_1 &= r \cos(\phi_1), \\ w_2 &= r \sin(\phi_1) \cos(\phi_2), \\ &\vdots \\ w_{d-1} &= r \sin(\phi_1) \cdots \sin(\phi_{d-2}) \cos(\phi_{d-1}), \\ w_d &= r \sin(\phi_1) \cdots \sin(\phi_{d-2}) \sin(\phi_{d-1}), \end{aligned} \quad (\text{C.1})$$

for $q \in \mathbb{R}$, $r > 0$, $\phi_1, \dots, \phi_{d-2} \in [0, \pi]$, and $\phi_{d-1} \in [0, 2\pi]$. The signed distance from Section 2 becomes

$$d_{\mathcal{M}}(\mathbf{x}) = r[q + \cos(\phi_1)x^1 + \cdots + \sin(\phi_1) \cdots \sin(\phi_{d-1})x^d]. \quad (\text{C.2})$$

This substitution factorizes the sigmoid scaling r . If we use the polar parametrization, one needs to multiply the gradient matrix from Appendix B on the left by the transposed Jacobian of (C.1).

References

- [1] C. Cortes, X. Gonzalvo, V. Kuznetsov, M. Mohri, and S. Yang, “Adanet: Adaptive structural learning of artificial neural networks,” 2016.
- [2] R. M. Palnitkar and J. Cannady, “A review of adaptive neural networks,” in *IEEE SoutheastCon, 2004. Proceedings.*, pp. 38–47, March 2004.
- [3] C. Cortes, X. Gonzalvo, V. Kuznetsov, M. Mohri, and S. Yang, “Adanet: Adaptive structural learning of artificial neural networks,” *CoRR*, vol. abs/1607.01097, 2016.
- [4] D. Fink, “A compendium of conjugate priors,” 1997.
- [5] P. E. Pope, S. Kolouri, M. Rostami, C. E. Martin, and H. Hoffmann, “Explainability methods for graph convolutional neural networks,” in *Proceedings of the IEEE Conference on Computer Vision and Pattern Recognition*, pp. 10772–10781, 2019.
- [6] N. Frosst and G. E. Hinton, “Distilling a neural network into a soft decision tree,” *CoRR*, vol. abs/1711.09784, 2017.
- [7] R. Tanno, K. Arulkumaran, D. C. Alexander, A. Criminisi, and A. V. Nori, “Adaptive neural trees,” *CoRR*, vol. abs/1807.06699, 2018.
- [8] V. Medina-Chico, A. Suárez, and J. F. Lutsko, “Backpropagation in decision trees for regression,” in *Machine Learning: ECML 2001* (L. De Raedt and P. Flach, eds.), (Berlin, Heidelberg), pp. 348–359, Springer Berlin Heidelberg, 2001.
- [9] G. Biau, E. Scornet, and J. Welbl, “Neural random forests,” *Sankhya A*, 04 2016.
- [10] S. R. Bulò and P. Kontschieder, “Neural decision forests for semantic image labelling,” in *Proceedings of the 2014 IEEE Conference on Computer Vision and Pattern Recognition, CVPR ’14*, (Washington, DC, USA), pp. 81–88, IEEE Computer Society, 2014.
- [11] D. Bertsimas and J. Dunn, “Optimal classification trees,” *Machine Learning*, vol. 106, pp. 1039–1082, Jul 2017.
- [12] J. F. G. de Freitas, *Bayesian methods for neural networks*. PhD thesis.

- [13] C. Blundell, J. Cornebise, K. Kavukcuoglu, and D. Wierstra, “Weight uncertainty in neural network,” in *Proceedings of the 32nd International Conference on Machine Learning* (F. Bach and D. Blei, eds.), vol. 37 of *Proceedings of Machine Learning Research*, (Lille, France), pp. 1613–1622, PMLR, 07–09 Jul 2015.
- [14] V. Mullachery, A. Khera, and A. Husain, “Bayesian neural networks,” 2018.
- [15] N. Chouikhi and A. M. Alimi, “Adaptive extreme learning machine for recurrent beta-basis function neural network training,” *CoRR*, vol. abs/1810.13135, 2018.
- [16] G. Nuti, L. A. Jiménez Rugama, and I. Cross, “A Bayesian Decision Tree Algorithm.” <https://arxiv.org/abs/1901.03214>, 2019.
- [17] D. E. Rumelhart, G. E. Hinton, and R. J. Williams, “Neurocomputing: Foundations of research,” pp. 696–699, 1988.
- [18] T. M. Cover, “Geometrical and statistical properties of systems of linear inequalities with applications in pattern recognition,” *Electronic Computers, IEEE Transactions on*, vol. EC-14, no. 3, pp. 326–334, 1965.
- [19] S. Dragomir, R. Agarwal, and N. Barnett, “Inequalities for beta and gamma functions via some classical and new integral inequalities,” *Journal of Inequalities and Applications*, vol. 5, 01 2000.
- [20] J. L. W. V. Jensen, “Sur les fonctions convexes et les inégalités entre les valeurs moyennes,” *Acta Mathematica*, vol. 30, pp. 175–193, Dec 1906.
- [21] B. D. Ripley, “Neural networks and related methods for classification,” *Journal of the Royal Statistical Society. Series B (Methodological)*, vol. 56, no. 3, pp. 409–456, 1994.
- [22] F. Pedregosa, G. Varoquaux, A. Gramfort, V. Michel, B. Thirion, O. Grisel, M. Blondel, P. Prettenhofer, R. Weiss, V. Dubourg, J. Vanderplas, A. Passos, D. Cournapeau, M. Brucher, M. Perrot, and E. Duchesnay, “Scikit-learn: Machine Learning in Python ,” *Journal of Machine Learning Research*, vol. 12, pp. 2825–2830, 2011.
- [23] O. Irsoy, O. T. Yildiz, and E. Alpaydin, “Budding trees,” in *International Conference on Pattern Recognition*, 2014.
- [24] R. K. Bock, “Major atmospheric gamma imaging cherenkov telescope project (magic).” <https://www.openml.org/d/1120>. Accessed: 2019-12-09.
- [25] M. Revow, “Ringnorm dataset.” <https://www.openml.org/d/1496>. Accessed: 2019-12-09.

- [26] M. Hopkins, E. Reeber, G. Forman, and J. Suermondt, “Spam e-mail database.” <https://www.openml.org/d/44>. Accessed: 2019-12-09.
- [27] M. Revow, “Twonorm dataset.” <https://www.openml.org/d/1507>. Accessed: 2019-12-09.